PHYSICAL REVIEW B **80**, 241308(R) (2009)

Microwave stabilization of edge transport and zero-resistance states

A. D. Chepelianskii[1] and D. L. Shepelyansky[2,3]
[1]*LPS, Université Paris-Sud, CNRS, UMR 8502, F-91405 Orsay, France*
[2]*Université de Toulouse, UPS, Laboratoire de Physique Théorique (IRSAMC), F-31062 Toulouse, France*
[3]*CNRS, LPT (IRSAMC), F-31062 Toulouse, France*

(Received 5 May 2009; revised manuscript received 24 November 2009; published 16 December 2009)

Edge channels play a crucial role for electron transport in two-dimensional electron gas under magnetic field. It is usually thought that ballistic transport along edges occurs only in the quantum regime with low filling factors. We show that a microwave field can stabilize edge trajectories even in the semiclassical regime leading to a vanishing longitudinal resistance. This mechanism gives a clear physical interpretation for observed zero-resistance states.

DOI: 10.1103/PhysRevB.80.241308 PACS number(s): 73.40.−c, 05.45.−a, 72.20.My

The experimental observation of microwave induced zero-resistance states (ZRSs) in high mobility two-dimensional electron gas (2DEG)[1,2] attracted significant experimental and theoretical interest. Several theoretical explanations have been proposed so far, which rely on scattering mechanisms *inside the bulk of 2DEG*. The "displacement" mechanism originates from the effect of microwaves on disorder elastic scattering in the sample,[3] while the "inelastic" mechanism involves inelastic processes that lead to a modified out-of-equilibrium distribution function.[4] Even if these theories reproduce certain experimental features we believe that the physical origin of ZRS is still not captured. Indeed, the above theories naturally generate negative resistance states but one has to rely on an uncontrolled out-of-equilibrium compensation of all currents to produce ZRS as observed in experiments.[1,2] Also ZRSs appear in very clean samples where in the bulk an electron moves like an oscillator and selection rules allow transitions only between nearby oscillator states. Hence resonant transitions are possible only at cyclotron resonance where the ratio j between microwave frequency ω and cyclotron frequency ω_c is unity. But experiments show that the onset of ZRS occurs also for high $j=\omega/\omega_c$ approximately at $j=1+1/4, 2+1/4, \ldots$. High j resonances could appear due to nonlinear effects, however the microwave fields are relatively weak giving a ratio ϵ between oscillating component of electron velocity and Fermi velocity v_F of the order of few percent. Thus in these theories, high j ZRS can only be explained by assuming the presence of a short range disorder potential. However the main sources of elastic scattering in 2DEG are ionized impurities in the remote doping layer which creates a smooth potential landscape.[5,6]

In order to develop a theory valid for smooth disorder, we note that ZRSs occur when the mean free path l_e is much larger than the cyclotron radius $r_c=v_F/\omega_c$. In usual 2DEG samples with lower mobilities this regime corresponds to strong magnetic fields and quantum Hall effect. In this case it is known that propagation along sample edges is ballistic and plays a crucial role in magnetotransport. It leads to quantization of the Hall resistance R_{xy} and to the disappearance of four terminal resistance R_{xx} strikingly similar to ZRS.[7] This occurs at low filling factors ν when a gap forms in the 2DEG density of states due to discreetness of Landau levels. In contrast to that ZRSs appear at $\nu \simeq 50$ where Landau levels are smeared out by smooth disorder. Inside the bulk with a smooth disorder length scale $l_d \gg r_c$ the adiabatic and Kolmogorv-Arnold-Moser (KAM) theorems give an exponential drop of both the diffusion rate and high j microwave harmonics $\propto \exp[-(j-1)l_d/r_c]$ at $j>1$ (see, e.g., Ref. 8). Thus in this semiclassical regime, edge trajectories become dominant for transport. Guiding along sample edges can lead to a significant decrease of R_{xx} with magnetic fields giving a negative magnetoresistance and singularities in R_{xy} (Refs. 9 and 10) (note that negative magnetoresistance is also observed in ZRS samples[1,2,11]). This behavior can be understood theoretically from the transmission probability T between voltage probes in a Hall bar geometry.[10] The drop in R_{xx} is linked to increased T, but transmission remains smaller than unity due to disorder and R_{xx} remains finite. Recently this model was extended to understand experimental deviations from Onsager reciprocity relations in samples under microwave driving.[12] But the impact of microwaves on stability of edge channels was never considered before.

In this Rapid Communication we show that microwave radiation can stabilize guiding along sample edges leading to a ballistic transport regime with vanishing R_{xx} and transmission exponentially close to unity. It was established experimentally that edge channels are very sensitive to irradiation[13] and recent contactless measurements in the ZRS regime did not show a significant drop of R_{xx} (Ref. 14) that supports our edge transport mechanism for ZRS. Our model also relies on the fact that scattering occurs on small angles in 2DEG.[1,15] This contrasts with other ZRS models which do not rely on specific physical properties of 2DEG.

Since filling factors are large we study classical dynamics of an electron at the Fermi surface[10] propagating along a sample edge modeled as a specular wall. The motion is describe by Newton equations,

$$d\mathbf{v}/dt = \boldsymbol{\omega}_\mathbf{c} \times \mathbf{v} + \epsilon\omega \cos \omega t - \gamma(v)\mathbf{v} + I_{wall} + I_S, \qquad (1)$$

where $\epsilon = e\mathbf{E}/(m\omega v_F)$ describes microwave driving field $\mathbf{E}$, velocity is measured in units of Fermi velocity v_F, and $\gamma(v)=\gamma_0(|\mathbf{v}|^2-1)$ describes relaxation processes to the Fermi surface. The last two terms account for elastic collisions with the wall and small angle scattering. Disorder scattering is

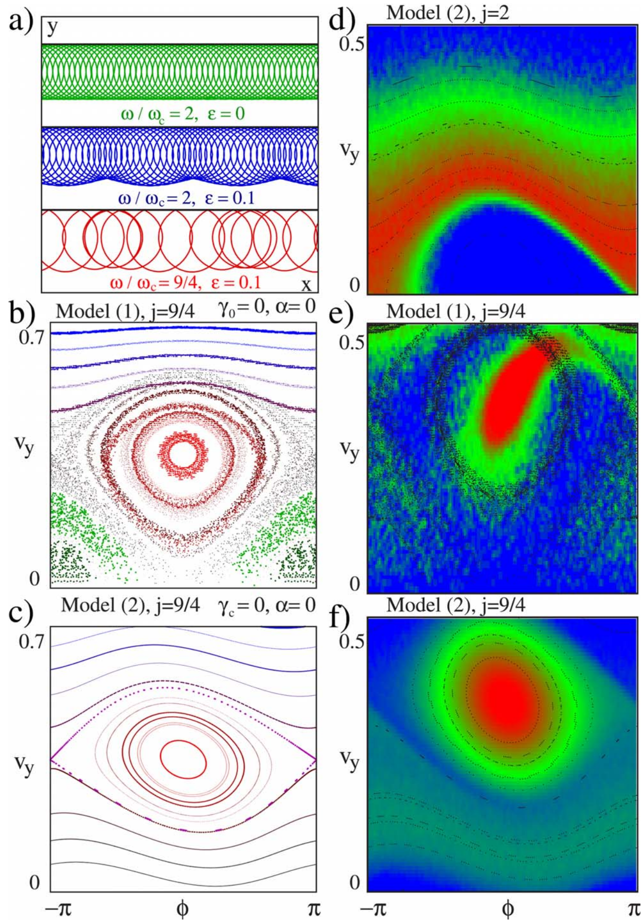

FIG. 1. (Color online) (a) Examples of electron trajectories along sample edge for several values of $j=\omega/\omega_c$ and y-polarized field ϵ. (b) Poincaré section of Eq. (1) for $\omega/\omega_c=9/4$ at y polarized $\epsilon=0.02$. (c) Poincaré section in the same region for the map (2) giving approximate description of dynamics in (b). In (a)–(c) dissipation and impurity scattering angle are zero. (d)–(f) Density of propagating particles on the Poincaré section in presence of noise and dissipation [red/gray for maximum and blue/black for zero: in (d) maximal density is concentrated along the curve $v_y \approx 0.2\cos^2\phi/2$ and in (e) and (f) minimum is inside oval dashed curves with the center around $v_y\approx 0.4$, $\phi=0$]; black points show trajectories without noise and dissipation. (d) For $\omega/\omega_c=2$ microwave repels particles from the edge, (e) and (f) while for $\omega/\omega_c=9/4$ particles are trapped inside the nonlinear resonance. Here (e) $\gamma_0=10^{-3}$ and (d) and (f) $\gamma_c=10^{-2}$ and $\alpha\simeq 5\times10^{-3}$.

modeled as random rotations of $\mathbf{v}$ by small angles in the interval $\pm\alpha$ with Poissonian distribution over microwave period. Examples of electron dynamics along the sample edge for $\gamma_0=0$ and $\alpha=0$ are shown in Fig. 1(a). They show that even a weak field $\epsilon=0.1$ has strong impact on dynamics along the edge. A more direct understanding of the dynamics can be obtained from the Poincaré sections constructed for the microwave field phase $\phi=\omega t (\mathrm{mod}\, 2\pi)$ and the velocity component $v_y>0$ at the moment of collision with the wall. The system [Eq. (1)] has two and half degrees of freedom and therefore the curves on the section are only approximately invariant [Fig. 1(b)]. The main feature of this figure is the appearance of a nonlinear resonance. We assume for simplicity that 2DEG is not at cyclotron resonance and polarization is mainly along y axis. Since Eq. (1) is linear outside the wall, one can go to the oscillating frame where electron moves on a circular orbit while the wall oscillates in y with velocity $\epsilon \sin \omega t$. Hence collisions change v_y by twice the wall velocity. For small collision angles the time between collisions is $\Delta t=2(\pi-v_y)/\omega_c$. This yields an approximate dynamics description in terms of the Chirikov standard map,[8]

$$\bar{v}_y = v_y + 2\epsilon \sin\phi + I_{cc}, \quad \bar{\phi} = \phi + 2(\pi-\bar{v}_y)\omega/\omega_c. \quad (2)$$

The term $I_{cc}=-\gamma_c v_y+\alpha_n$ describes dissipation and noise and bars denote values after map iteration $(-\alpha<\alpha_n<\alpha)$. Damping from electron-phonon and electron-electron collisions contributes to γ_c. The Poincaré sections for Eqs. (1) and (2) are compared in Figs. 1(b) and 1(c) showing that the Chirikov standard map gives a good description for edge dynamics under microwave driving. A phase shift by 2π does not change the behavior of map [Eq. (2)] and hence the phase space structure is periodic in $j=\omega/\omega_c$ with period unity which naturally yields high harmonics. The resonance is centered at $v_y=\pi(1-m\omega_c/\omega)$, where m is the integer part of ω/ω_c. The chaos parameter of the map is $K=4\epsilon\omega/\omega_c$ and the resonance separatrix width $\delta v_y=4\sqrt{\epsilon\omega_c/\omega}$. The energy barrier of the resonance is given by $E_r=(\delta v_y)^2/2=8\epsilon\omega_c/\omega$.

In presence of weak dissipation the center of resonance acts as an attractor for trajectories inside the resonance. The presence of small angle scattering leads to a broadening of the attractor but trajectories are still trapped inside. If the center is located near $v_y=0$ particles are easily kicked out from the edge, transmission T drops, and R_{xx} increases. On the other hand, if the resonance width δv_y does not touch $v_y=0$ then orbits trapped inside propagate ballistically with $T\to 1$ and $R_{xx}\to 0$. The trapping is confirmed in Figs. 1(e) and 1(f) for both models at $\omega/\omega_c=9/4$ with propagating trajectories concentrated inside the resonance, whereas for $\omega/\omega_c=2$ in Fig. 1(d) the region inside the resonance does not propagate (propagating orbits concentrate on the unstable separatrix and their number is much smaller).

In order to compare our theory with experiment we calculate the transmission T for model (1). An ensemble of $N=5000$ particles is thrown on the wall at $x=0$ with random velocity angle. They propagate in positive x direction but due to noise some trajectories detach from the wall; we consider that a particle is lost in the bulk when it does not collide with the wall for time $20\pi/\omega_c$. These particles do not contribute to transmission which is defined as the fraction of particles that reaches $x=250v_F/\omega$, which can be viewed as a distance between contacts. For $l_e \gg r_c$ the billiard model of a Hall bar[10,12] gives $R_{xx}\propto 1-T$ and a deviation from the classical Hall conductance $\Delta R_{xy}=R_{xy}-B/ne\propto -(1-T)$. The four terminal resistance $R_{xx}\propto 1-T$ can also be obtained as the inverse of the four terminal Landauer conductance $G_{xx}\propto T/(1-T)$ with T close to unity.[16] The data in Fig. 2 show calculated $1-T$ and experimental R_{xx} and ΔR_{xy}.[2] One can see a good agreement between results of model (1) and experimental data. Both show R_{xx} peaks at integer j and zeros around $j=5/4, 9/4, \ldots$. We also reproduce peaks and dips for "fractional" ZRS around $j=3/2, 1/2$.[17] Our specular wall potential is specially suited for the cleaved samples from

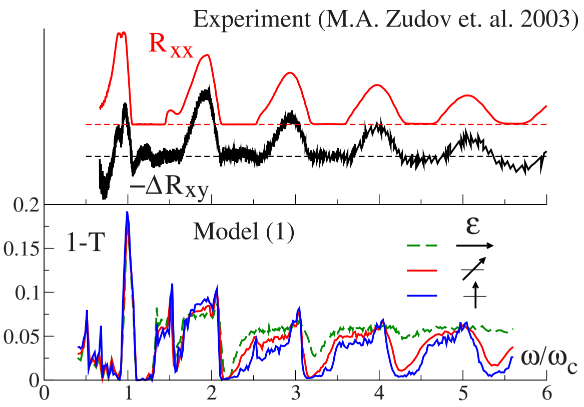

FIG. 2. (Color online) Top panel: dependence of R_{xx} and $-\Delta R_{xy}$ (in arbitrary units) on ω/ω_c from Ref. 2. ΔR_{xy} is obtained from measured Hall resistance by subtracting a linear fit to R_{xy}. Bottom panel: calculated transmission along sample edge for three microwave polarization axes. Microwave field is $\epsilon=0.05$, relaxation $\gamma_0=10^{-3}$, and noise amplitude $\alpha=3\times10^{-3}$. Transmission without microwaves is $T\simeq0.95$.

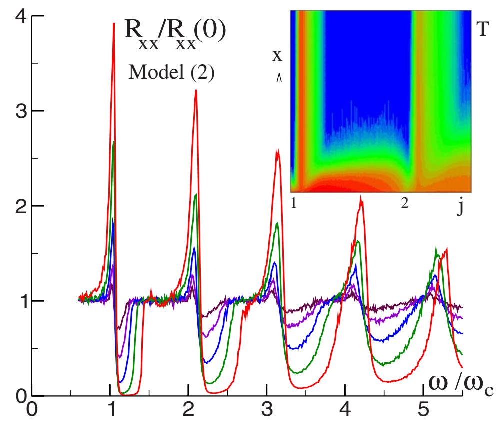

FIG. 3. (Color online) Dependence of rescaled R_{xx} in model (2) on ω/ω_c for microwave fields $\epsilon=0.00375$, 0.0075, 0.015, 0.03, and 0.06 (curves from top to bottom at $j=\omega/\omega_c=4.5$); $\gamma_c=0.01$, $\alpha=0.03$. Average is done over 10^4 particles and 5000 map iterations. The inset shows transmission probability T at distance x along the edge for $\epsilon=0.02$ (red/gray is for maximum and blue/black for zero, $0<x<10^3 v_F/\omega$).

Ref. 2 where edges should follow crystallographic directions but peak positions can be shifted for other edge potentials. We also note that the possibility to observe ZRS on ΔR_{xy} was discussed in Ref. 18. The four terminal resistance $R_{xx}\propto1-T$ can also be obtained as the inverse of the four terminal Landauer conductance $G_{xx}\propto T/(1-T)$ with T close to unity Finally our data show weak dependence on polarization axis which supports the Chirikov standard map model.

Model (2) is more accessible to analytical analysis and numerical simulations. In this model a particle is considered lost in the bulk as soon as $v_y<0$. The displacement along the edge between collisions is $\delta x=2v_y/\omega_c$ and an effective "diffusion" along the edge is defined as $D_x(\epsilon)=(\Delta x)^2/\Delta t$, where Δx is a total displacement along the edge during the computation time $\Delta t\sim10^4/\omega$. In numerical simulations D_x is averaged over 10^4 particles homogeneously distributed in phase space. We then assume that $R_{xx}\propto1/D_x$ and present the dependence of the dimensionless ratio $R_{xx}/R_{xx}(\epsilon=0)$ on ω/ω_c in Fig. 3. The computation of transmission T (shown in Fig. 3, inset) gives similar results but is less convenient for numerical analysis. The dependence on $j=\omega/\omega_c$ is similar to those shown in Fig. 2. Both peaks and dips grow with the increase of microwave field ϵ.

The dependence on ϵ can be understood from the following arguments. Due to noise a typical spread square width in velocity angle during the relaxation time $1/\gamma_c$ is $D_s=\alpha^2/\gamma_c$. The resonance square width is $(\delta v_y)^2=16\epsilon\omega_c/\omega$ and therefore the probability to escape from the resonance is

$$W\sim\exp[-(\delta v_y)^2/D_s]\sim\exp[-A\epsilon\omega_c/(D_s\omega)]. \qquad (3)$$

Edge transport is ballistic for exponentially small W and $R_{xx}/R_{xx}(0)\sim1-T\sim W$. The above estimate gives the numerical coefficient $A=16$ while numerical data presented in Fig. 4 for model (2) give $A\approx12$ and confirm dependence [Eq. (3)] on all model parameters. It holds when edge transport is stabilized by the presence of the nonlinear resonance which corresponds to regions around $j=5/4,9/4,\ldots$. Deviations appear when the parameter $K=4\epsilon\omega/\omega_c$ approaches the chaos border $K\approx1$ and trapping is weakened by chaos. The numerical data for model (1) based on transmission computation confirm the scaling dependence $\log_{10}R_{xx}/R_{xx}(0)\propto-\omega_c\epsilon/\omega$ as shown in Fig. 4. This dependence holds also for other models of dissipation in Eqs. (1) and (2). It is consistent with the power dependence measured in Ref. 1. A detailed analysis of the power dependence may be complicated due to heating and out-of-equilibrium effects at strong power, but the global exponential decay of R_{xx} with power was confirmed in Ref. 18.

The billiard model used in our studies focuses on dynamics of an electron on the Fermi surface which corresponds to a zero temperature limit. In order to include the effect of temperature T_e one needs to account for the thermal smearing of the electrons around the Fermi surface. The relaxation rate to the Fermi surface that we introduced in our model is

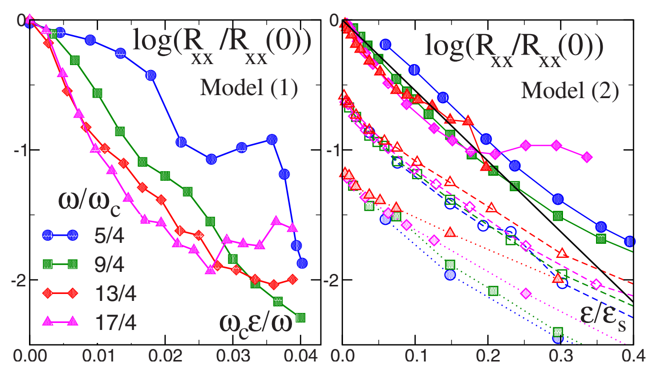

FIG. 4. (Color online) Dependence of rescaled R_{xx} on rescaled microwave field ϵ for models (1) (left) and (2) (right). Left: parameters as in Fig. 2 and ϵ is varied. Right: $\gamma=0.01$, $\alpha=0.02$ (full curves), $\gamma=0.01$, $\epsilon=0.03$ (dashed curves), $\epsilon=0.03$, $\alpha=0.02$ (dotted curves), and the straight line shows theory [Eq. (3)] with $A=12.5$; symbols are shifted for clarity and $\epsilon_s=\omega D_s/\omega_c$. Logarithms are decimal.

also likely to depend on temperature. This makes rigorous analysis of temperature dependence challenging. A simple estimate can be obtained in the frame of Arrhenius law with activation energy equals the energy height of the nonlinear resonance $E_r = 16\epsilon\omega_c E_F/\omega$, where E_F is the Fermi energy. This dependence appears as an additional damping factor in ZRS amplitude in a way similar to temperature dependence of Shubnikov–de Hass oscillations leading to

$$R_{xx} \propto \exp[-A\epsilon\omega_c/(D_s\omega)]\exp(-16\epsilon\omega_c E_F/\omega T_e). \quad (4)$$

Our prediction on activation energy E_r is in a good agreement with experimental data and reproduces the proportionality dependence on magnetic field observed in Refs. 1 and 2. For a typical $\epsilon = 0.01$ we obtain $E_r \sim 20$ K at $j=1$. The proposed mechanism can find applications for microwave induced stabilization of ballistic transport in magnetically confined quantum wires.[19]

In summary we have shown that microwave radiation can stabilize edge trajectories against small angle disorder scattering. For propagating edge channels a microwave field creates a nonlinear resonance well described by the Chirikov standard map. Dissipative processes lead to trapping of particle inside the resonance. Depending on the position of the resonance center with respect to the edge the channeling of particles can be enhanced or weakened providing a physical explanation of ZRS dependence on the ratio between microwave and cyclotron frequencies. In the trapping case transmission along the edges is exponentially close to unity, naturally leading to an exponential drop in R_{xx} with microwave power. Our theory also explains the appearance of large energy scale in temperature dependence of ZRS. A complete theory should perform a microscopic treatment of dissipation and take into account quantum effects since about ten Landau levels are typically captured inside the resonance.

Recently, an experiment[20] showed that in short ZRS samples the maxima of R_{xx} persist but the minima are washed out. This fits well our theory where maxima appear after the short time of one rotation around the nonlinear resonance while minima are established after the long relaxation time of orbits trapped inside the resonance (see Fig. 3, inset). Also experiments with electrons on liquid helium surface[21] show ZRS-like oscillations supporting the classical origin of the effect with smooth disorder as discussed here.

We are grateful to H. Bouchiat, A. A. Bykov, and A. S. Pikovsky for fruitful discussions. This research was supported in part by the ANR PNANO project NANOTERRA. A.D.C. acknowledges DGA for support.

[1] R. G. Mani, J. H. Smet, K. von Klitzing, V. Narayanamurti, W. B. Johnson, and V. Umansky, Nature (London) **420**, 646 (2002).
[2] M. A. Zudov, R. R. Du, L. N. Pfeiffer, and K. W. West, Phys. Rev. Lett. **90**, 046807 (2003).
[3] V. I. Ryzhii, Sov. Phys. Solid State **11**, 2078 (1970); A. C. Durst, S. Sachdev, N. Read, and S. M. Girvin, Phys. Rev. Lett. **91**, 086803 (2003); M. G. Vavilov and I. L. Aleiner, Phys. Rev. B **69**, 035303 (2004); J. Iñarrea and G. Platero, Phys. Rev. Lett. **94**, 016806 (2005).
[4] I. A. Dmitriev, A. D. Mirlin, and D. G. Polyakov, Phys. Rev. Lett. **91**, 226802 (2003); I. A. Dmitriev, M. G. Vavilov, I. L. Aleiner, A. D. Mirlin, and D. G. Polyakov, Phys. Rev. B **71**, 115316 (2005).
[5] H. L. Stormer, Surf. Sci. **132**, 519 (1983).
[6] T. Ando, J. Phys. Soc. Jpn. **51**, 3900 (1982).
[7] B. I. Halperin, Phys. Rev. B **25**, 2185 (1982); M. Büttiker, *ibid.* **38**, 9375 (1988).
[8] B. V. Chirikov, Phys. Rep. **52**, 263 (1979).
[9] M. L. Roukes, A. Scherer, S. J. Allen, Jr., H. G. Craighead, R. M. Ruthen, E. D. Beebe, and J. P. Harbison, Phys. Rev. Lett. **59**, 3011 (1987).
[10] C. W. J. Beenakker and H. van Houten, Phys. Rev. Lett. **63**, 1857 (1989).
[11] A. A. Bykov, A. K. Bakarov, D. R. Islamov, and A. I. Toropov, JETP Lett. **84**, 391 (2006).
[12] A. D. Chepelianskii and H. Bouchiat, Phys. Rev. Lett. **102**, 086810 (2009).
[13] R. Merz, F. Keilmann, R. J. Haug, and K. Ploog, Phys. Rev. Lett. **70**, 651 (1993).
[14] I. V. Andreev, V. M. Murav'ev, I. V. Kukushkin, J. H. Smet, K. von Klitzing, and V. Umanskii, Pis'ma Zh. Eksp. Teor. Fiz. **88**, 707 (2008) [JETP Lett. **88**, 616 (2008)].
[15] T. Ando, A. B. Fowler, and F. Stern, Rev. Mod. Phys. **54**, 437 (1982).
[16] S. Datta, *Electronic Transport in Mesoscopic Systems* (Cambridge University Press, Cambridge, 1995).
[17] M. A. Zudov, R. R. Du, L. N. Pfeiffer, and K. W. West, Phys. Rev. B **73**, 041303(R) (2006).
[18] R. G. Mani, V. Narayanamurti, K. von Klitzing, J. H. Smet, W. B. Johnson, and V. Umansky, Phys. Rev. B **69**, 161306(R) (2004); **70**, 155310 (2004).
[19] A. Nogaret, J.-C. Portal, H. E. Beere, D. A. Ritchie, and C. Phillips, J. Phys.: Condens. Matter **21**, 025303 (2009).
[20] A. A. Bykov, JETP Lett. **89**, 575 (2009).
[21] D. Konstantinov and K. Kono, EP2DS-18/MSS-14 Conference, Kobe, Japan, 2009 (unpublished).